



In vitro and *in vivo* evaluation of a dextran-graft-polybutylmethacrylate copolymer coated on CoCr metallic stent

Cécilia Delattre^{1*}, Diego Velasquez¹, Caroline Roques^{1,2}, Graciela Pavon-Djavid^{1,2}, Véronique Ollivier^{1,2}, Anna Lokajczyk^{3,4}, Thierry Avramoglou^{1,2}, Virginie Gueguen^{1,2}, Liliane Louedec^{1,2}, Giuseppina Caligiuri^{1,2}, Martine Jandrot-Perrus^{1,2}, Catherine Boisson-Vidal^{3,4}, Didier Letourneur^{1,2} and Anne Meddahi-Pelle^{1,2}

¹INSERM, UMR_S1148, Laboratory for Vascular Translational Sciences, Hôpital Bichat

²Université Paris 13, Sorbonne Paris Cité, France

³Inserm UMR_S1140, Paris France

⁴Université Paris Descartes, Sorbonne Paris Cité, France

Article Info



Article Type:

Original Article

Article History:

Received: 29 May 2018

Revised: 17 Sep. 2018

Accepted: 24 Sep. 2018

ePublished: 2 Oct. 2018

Keywords:

Animal model
 Biocompatibility
 Dextran
 Haemocompatibility
In vitro
 Stent

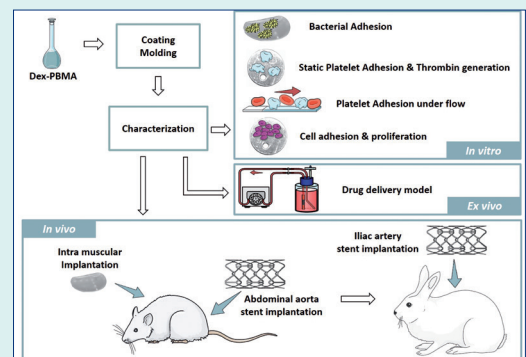
Abstract

Introduction: The major complications of stent implantation are restenosis and late stent thrombosis. PBMA polymers are used for stent coating because of their mechanical properties. We previously synthesized and characterized Dextran-graft-polybutylmethacrylate copolymer (Dex-PBMA) as a potential stent coating. In this study, we evaluated the haemocompatibility and biocompatibility properties of Dex-PBMA *in vitro* and *in vivo*.

Methods: Here, we investigated: (1) the effectiveness of polymer coating under physiological conditions and its ability to release Tacrolimus®, (2) the capacity of Dex-PBMA to inhibit *Staphylococcus aureus* adhesion, (3) the thrombin generation and the human platelet adhesion in static and dynamic conditions, (4) the biocompatibility properties *in vitro* on human endothelial colony forming cells (ECFC) and on mesenchymal stem cells (MSC) and *in vivo* in rat models, and (5) we implanted Dex-PBMA and Dex-PBMA_{TAC} coated stents in neointimal hyperplasia restenosis rabbit model.

Results: Dex-PBMA coating efficiently prevented bacterial adhesion and release Tacrolimus®. Dex-PBMA exhibit haemocompatibility properties under flow and ECFC and MSC compatibility. *In vivo*, no pathological foreign body reaction was observed neither after intramuscular nor intravascular aortic implantation. After Dex-PBMA and Dex-PBMA_{TAC} coated stents 30 days implantation in a restenosis rabbit model, an endothelial cell coverage was observed and the lumen patency was preserved.

Conclusion: Based on our findings, Dex-PBMA exhibited vascular compatibility and can potentially be used as a coating for metallic coronary stents.



Introduction

Percutaneous transluminal coronary angioplasty followed by a stent implantation is the first technique of the revascularization. Most of these stents are manufactured using cobalt chromium coated with iridium oxide or diamond-like carbon layers to prevent the formation of an oxide layer on their surface that is fragile and mechanically unstable under flow conditions.¹ Despite the development of new coronary stent technologies, interactions of blood

and cells with the implanted devices remain a serious cause of side effects. The major complications of their implantation are restenosis and late stent thrombosis (LST), which raises serious questions about their long-term safety. In-stent restenosis results from the proliferation of smooth muscle cells (SMCs).² Late thrombus formation mechanism has not been fully explained yet, nevertheless, LST is thought to be associated with premature cessation of antiplatelet therapy in patients, stent malapposition,



*Corresponding author: Cécilia Delattre, Email: cecilia.delattre@gadz.org



© 2019 The Author(s). This work is published by BioImpacts as an open access article distributed under the terms of the Creative Commons Attribution License (<http://creativecommons.org/licenses/by-nc/4.0/>). Non-commercial uses of the work are permitted, provided the original work is properly cited.

late re-endothelialization of the stent struts and the nature of polymer coating.³⁻⁶ In 45% of cases, they lead to patient death.

In this context, three main approaches were developed to design safer drug-eluting stent (DES).⁷ The first one is polymer-free coating.⁸⁻¹⁰ Stent surfaces are microporous or contain cavities where drugs are loaded. Nevertheless, the release control on these stents is difficult and the velocity is often too high.^{8,11,12} The second one consists of a biodegradable polymer coating that allows the drug-delivery during the degradation of the polymer.^{10,13} In this case, the polymer and its degradation products have to be biocompatible and not trigger any inflammatory reactions. Many biodegradable coatings were investigated.^{14,15} Alternatively, biodegradable stents were also developed.^{11,16,17} Nevertheless, side effects such as inflammatory reactions related to their degradation products have been reported.¹⁵ Clinical studies revealed that these bioresorbable stents led to an increased risk of stent thrombosis in comparison with DES. As a matter of fact, metallic stents appear to be the most adapted device to prevent coronary artery closure. The third approach is therefore based on a non-degradable polymer that protects the stent from corrosion. In vitro metallic stent backbone was shown to release degradation products leading to a possible allergic reaction or sensitization.¹⁸ The polymer must be biocompatible and should promote endothelial coverage to prevent side effects in contact with blood.⁵ Recent studies suggest that the faster the re-endothelialisation of the stented area is, the lower the risks of inflammation and thrombus formation are.¹⁹ The drug action and the polymeric coating materials themselves may inhibit the growth of endothelial cells, leading to disturbed vascular healing.²⁰ In this context, it was stated that the stent platform, the drug and the polymeric drug carrier are all targets for DES improvement.¹⁹

Polymethacrylate polymers are widely used on medical devices for their mechanical properties and particularly the poly(*n*-butylmethacrylate) (PBMA) on several DES.²¹ Nonetheless, it is associated with another polymer because if the polymer is used on its own, its elasticity is too low to resist to stent deformation.^{21,22} Previous works have demonstrated that a copolymer of dextran, a natural polysaccharide, along with PBMA (Dex-PBMA) exhibits elastic properties suitable for stent coating.²² This combination promotes in vitro endothelial cell growth and inhibits the SMCs proliferation compared to PBMA alone.²³ Besides, dextran is non-toxic and has already been approved by the US Food and Drug Administration for its clinical use for example as plasma volume expander.²⁴

Therefore this study was undertaken to evaluate the haemocompatibility and biocompatibility of Dex-PBMA coated on glass coverslips and CoCr discs or stents, *in vitro* on coagulation, platelets and endothelial cells. Then more studies were performed *ex vivo* and *in vivo* in preclinical models of restenosis and intimal hyperplasia.

Material and Methods

Materials

Dextran (70 kg.mol⁻¹) and FK-506 monohydrate (Tacrolimus TAC) were purchased from Sigma-Aldrich (St Quentin Fallavier, France). Butylmethacrylate (BMA) monomers, ceric ammonium nitrate and nitric acid were obtained from Acros (Illkirch, France). BMA monomers were purified by washing with NaOH (5%) and NaCl (20%) followed by distilled water three times. The coating was performed on electropolished CoCr disks (L615) 5 mm in diameter and 0.5 mm thick and onto CoCr stents from Abbott Vascular (Rungis, France).

Dextran-PBMA copolymer synthesis and characterization

Copolymerization

The Dextran-PBMA copolymer (Dex-PBMA) synthesis was adapted from Derkaoui et al.²³ Briefly, the reactions were carried out in a 1 L five-neck flask equipped with stirrer and condenser. The flask was immersed in a thermostated oil bath at 40°C and purged by nitrogen gas. Then 0.125 g of dextran was dissolved in 500 mL of 0.05 M HNO₃ for 10 min. Then, 5 mL of the solution of ceric ammonium nitrate dissolved in 0.2 M HNO₃ (0.24 mM) and 2 g of BMA monomers were simultaneously added. After 40 min agitation, the pH was adjusted to 8 by the addition of 10 M NaOH aqueous solution and the solution was then concentrated in a rotavapor. The Dex-PBMA was precipitated in methanol and washed with 50 mL EDTA (10⁻² M) to remove cerium, then lyophilized. To remove free PBMA homopolymer, the resulting product was extracted in acetone in a continuous extraction system (Soxhlet) for 6 hours, lyophilized and the Dex-PBMA powder was stored at room temperature. Twelve syntheses were performed and mixed to obtain a sufficient quantity of Dex-PBMA to carry experiments with a homogeneous batch.

Dex-PBMA coating and Dex-PBMA film preparation

Dex-PBMA polymer were coated either on glass coverslips, CoCr discs or CoCr stents, or prepared as a film. For that purpose, Dex-PBMA was dissolved in tetrahydrofuran (THF) and H₂O at a ratio of 92:8 (v/v). Then 50 µL or 1000 µL of a 30% (w/v) copolymer solution were loaded at the surface of a CoCr disc or glass coverslip, respectively, and left to evaporation 24 hours at room temperature in a saturated atmosphere of THF in the presence of CaCl₂ to absorb water. After drying (24 hours, 37°C) and UV sterilization, coated disc (Dex-PBMA disc) or coated-glass coverslip were rinsed with phosphate buffered saline solution (PBS).

The stents, after deployment were dip-coated by immersion in a 20% (w/v) copolymer solution, evaporated in the presence of THF and CaCl₂, dried 24 hours at 37°C, UV sterilized and washed in a saline solution (NaCl 0.9%). The Dex-PBMA-coated stents (Dex-PBMA stent) were mounted over a balloon and hand-crimped.

For film preparation, 1.5 mL of 30% (w/v) of copolymers solution was poured into a 15 mm diameter Petri dishes. After solvent evaporation, drying and sterilization were performed in the same experimental conditions as described above. An 8 mm diameter circular punch purchased from Harris, Uni-Core (Redding, USA) was used to obtain round-shaped films. Then, Dex-PBMA films were washed in NaCl 0.9%.

For disc and stent associated with Tacrolimus (Dex-PBMATAC disc or stent), TAC (1 mg.mL⁻¹) was dissolved in THF/water solution before Dex-PBMA in order to obtain Dex-PBMA_{TAC} solution. Then, disc or stent was coated in the same way as Dex-PBMA disc or stent.

Evaluation of Dex-PBMA coating resistance under flow conditions

The coating resistance of Dex-PBMA stent was evaluated in vitro under dynamic conditions. For that purpose, Dex-PBMA stents (internal expanded diameter 4 mm, 8 mm long) were expanded in a silicon tube Versilic® (4 mm in internal diameter) from Nortec (St Etienne du Rouvray, France) and submitted to a coronary-physiological flow (shear rate 1000 s⁻¹) in water at 37°C (n=3). During the same time-course experiment, Dex-PBMA stents were left in static condition (water, 37°C). After 7 days, samples were metalized with 5 nM of gold and observed using an environmental scanning electron microscopy (ESEM, XL30 ESEM-FEG Philips) with an accelerating voltage of 20 kV at Hivac.

Water contact angle analysis

Contact angles were evaluated using the sessile drop method using a DSA 10 Kruss Instrument (Villebon-sur-Yvette, France). A 1 µL water droplet was dispensed on the surface, and the contact angle determination for each sample was the average value of ten measurements on different parts of the samples: CoCr discs, Dex-PBMA discs and Dex-PBMA_{TAC} discs (n=3).

Biocompatibility tests

Blood collection and platelet isolation

Human whole blood was obtained from healthy volunteers exempt from medication for at least 10 days, after full informed consent was obtained, according to the Declaration of Helsinki. All experiments were carried out with fresh peripheral blood provided by the French blood bank institute (EFS) under an agreement with the INSERM U1148 (n°12/EFS/079). Blood was collected via venipuncture into siliconized Vacutainer™ tubes from Becton Dickinson (Le Pont de Claix, France) containing buffered sodium citrate (0.12 M, nine parts blood to one part sodium citrate solution) with the first tube being discarded. Whole blood was centrifuged at 120 g for 15 minutes at room temperature to prepare platelet-rich plasma (PRP). For thrombin generation, platelet counts in PRP were adjusted to the desired concentration by dilution with autologous platelet poor plasma (PPP).

PPP was prepared by centrifugation of the blood at 2,000 g for 15 minutes. Alternatively, blood was collected on acid-citrate-dextrose anticoagulant (ACD-A) to prepare washed platelets as previously reported.²⁵

Cell isolation and preparation

Human endothelial colony-forming cells (ECFCs) were isolated from human umbilical cord blood after the consent of mothers and the approval by the Biological Resources Center in the Cell Therapy Unit from Saint Louis Hospital (Paris, France), authorized by French Ministry of Research under number AC-2008-376 and certified by the French Normalization Agency under number 201/51848.1. ECFCs were expanded in Endothelial Cell Growth Medium EGM2 from Ozyme (Montigny-Le-Bretonneux, France) and characterized as previously described.²⁶ The presence of Weibel-Palade bodies, combined with the expression of endothelial markers (CD31, KDR, Tie-2, CD144), and dual positivity for DiI-AcLDL uptake and BS-1 lectin binding confirmed the endothelial phenotype of the ECFCs thus obtained. ECFCs do not express leukomonocytic markers such as CD45 and CD14. FACS analysis (FACS Calibur) from Becton Dickinson (Le Pont de Claix, France) was used to assess expression of endothelial-lineage cell surface antigens.²⁶ Cells were used with cells culture for less than 30 days.

Mesenchymal stem cells (MSCs) were isolated from bone marrow samples obtained after informed consent according to approved institutional guidelines (Assistance Publique-Hôpitaux de Paris, Paris, France). The bone marrow mononuclear cells were collected from ficoll gradients and cultured in minimum essential medium- α (MEM) from Invitrogen, ThermoFisher Scientific (Villebon sur Yvette, France), supplemented with 10% Foetal Calf Serum (FCS) from Gibco, ThermoFisher Scientific (Villebon sur Yvette, France), glutamax-I (2 mM) from Invitrogen, ThermoFisher Scientific (Villebon sur Yvette, France), basic Fibroblast Growth Factor FGF2 (1 ng.mL⁻¹) from R&D Systems (Abingdon, UK) and antibiotic/antimycotic (1%) from Invitrogen, ThermoFisher Scientific (Villebon sur Yvette, France). Cells were used between passage 4 and 7.

Static platelet adhesion on Dex-PBMA

Static evaluation of platelets adhesion was carried out on human washed platelets suspension (2.0 x 10⁸ platelets/mL) in reaction buffer (RB, NaCl 13.7 mM, KCl 0.1 mM, MgCl₂ 0.2 mM, Glucose 0.55 mM, HEPES 0.5 mM, NaH₂PO₄ 30 µM, NaHCO₃ 0.12 mM, BSA 3 mg.mL⁻¹, pH 7.3). Dex-PBMA or CoCr disks were loaded into wells of a 96 wells plate coated with 10 mg.mL⁻¹ of collagen type I (positive control, Horm collagen from Nycomed (Munich, Germany)) or 1% (w/v) of bovine serum albumin (BSA) in PBS. Washed platelets (20 000 000) were added into the wells and incubated for 1 hour at room temperature on a platform shaker. After two washes with RB, 100 µL of lysis solution (Na citrate 0.1 M, pNPP 1.3 mg.mL⁻¹, triton

X-100 20 $\mu\text{L}\cdot\text{mL}^{-1}$) were added for 1 hour 30 incubation at 37°C. The reaction was stopped with 25 μL of 1 M NaOH solution and supernatants were read at 405 nm (Fluostar Optima) from BMG Labtech (Champigny s/Marne, France). Each experiment was carried in three times and readings were made in duplicate. In order to observe the platelet morphology, Dex-PBMA or CoCr discs were fixed in 2.5% glutaraldehyde solution for 1 hour, dehydrated in ethanol and observed with Environmental Scanning Electron Microscopy (ESEM, XL30 ESEM-FEG Philips).

Dynamic platelet adhesion on Dex-PBMA

Dynamic evaluation of platelet adhesion was carried out on whole blood collected on 75 μM PPACK from Haematologic Technologies Inc. (Vermont, USA), then labelled with Dioc-6 (5 μM) from Interchim® (Montluçon, France) and perfused for 2 min at a shear rate of 1500 s^{-1} over Dex-PBMA or collagen-coated glass coverslip inserted in the flow chamber from Maastricht Instruments (Maastricht, Netherlands). All experiments (n=3) were observed in real-time and videotaped for off-line analysis. Quantification of fluorescent adherent platelets within time (t) was processed from digital images with ImageJ software using the t0 image as the zero reference.

Thrombin Generation on Dex-PBMA

Thrombin generation was measured in freshly prepared PRP (150 000 000 platelets. mL^{-1}) and PPP by means of the Calibrated Automated Thrombogram (CAT) method from Thromboscope BV (Maastricht, The Netherlands) as previously described.²⁷ Measurements were conducted with 80 μL PRP or PPP in a total volume of 120 μL in flat-bottom 96-well plates, containing Dex-PBMA and the CoCr discs. Thrombin generation was performed in the absence or presence of tissue factor (TF, 20 μL , 0.5 μM and 1 μM final concentration for PRP and PPP, respectively). Dedicated software from Thromboscope®, Thromboscope BV (Maastricht, The Netherlands) enables the calculation of thrombin activity and displays thrombin activity against time. All experiments were carried out 6 times. Results were expressed in a proportion of a control Immulon 2HB well from ThermoScientific® (Illkirch, France). The velocity index ($\text{nM}\cdot\text{min}^{-1}$) was calculated from CAT parameters [VI=Peak/(time to Peak-LagTime)]. LagTime (LT in min) is related to the initiation phase of coagulation and correspond to the generation of 10 nM of thrombin, time to Peak (tPeak in min) and Peak (maximal dose of thrombin produced in nM) are related to the amplification phase of coagulation.

Cell adhesion and proliferation on Dex-PBMA

One day before experiments, ECFCs and MSCs were growth-arrested for 18 h respectively in EBM2, 2.5% FCS and MEM Glutamax. They were then washed, detached with accutase from Sigma Aldrich (St Quentin Fallavier France) and suspended in the appropriate medium. All assays were performed in triplicate. Dex-PBMA or CoCr discs were placed at the bottom of 96-well plates. As a positive control some wells were coated with gelatin 0.2%

(30 μL , 20 min at RT). All samples were passivated with FCS (50 μL , 20 minutes at 37°C).

For cell adhesion assay, ECFCs or MSCs cells were seeded onto disc at 25 000 cell. cm^{-2} in the appropriate medium. The cells were incubated either for 20 minutes or 2 hours at 37°C in 5% CO₂ in a humidified incubator. After washing the disc with PBS to remove non-adherent cells, cell adhesion quantification was determined by pNPP from Sigma Aldrich (St Quentin Fallavier France) at 405 nM using a Fluostar optima from BMG Labtech (Champigny s/Marne, France).

For cell proliferation assay, ECFCs or MSCs cells were seeded on each disc at 15 000 cell. cm^{-2} in their respective media. The cells were incubated for 3 or 4 days at 37°C in 5% CO₂ in a humidified incubator. On day 3 and day 4, cell proliferation was evaluated by pNPP assay. In all assay, results were expressed as a ratio of gelatin control (n=3).

Bacterial adhesion on Dex-PBMA

The experimental procedure of the adhesion of *Staphylococcus aureus* CIP53136 obtained from Institut Pasteur (Paris, France) on Dex-PBMA film, CoCr disc and collagen (positive control) was adapted from Anagnostou et al.²⁸ *S. aureus* was used because it is the main bacteria involved in stent infection.²⁹

First, samples were incubated 1 hour at 37°C in FCS. The samples were then washed with PBS and then incubated with 1 mL of a suspension of *S. aureus* 108 colony forming units/ml (UFC/mL) concentration. After 1 hour of incubation at 37°C, samples were washed three times with PBS and incubated with 500 μL of trypsin. The removed bacteria were then spread on agar gel and cultivated overnight. Then, bacterial colonies were counted (n=3).

In vitro pharmacological drug-release studies

Dynamic perfusion systems were developed in order to study the release of a model molecule from the Dex-PBMA. The chosen molecule was tacrolimus (TAC). The circulation system was a flask containing perfusion medium - Dulbecco's Modified Eagles Medium (DMEM) from Invitrogen, ThermoFisher Scientific (Villebon sur Yvette, France) supplemented with sodium bicarbonate L-glutamine (2 mM, Invitrogen), penicillin/streptomycin (10 $\text{mL}\cdot\text{L}^{-1}$) from Gibco, ThermoFisher Scientific (Villebon sur Yvette, France) and FCS connected to a peristaltic pump and maintained at 37°C - in which one a stented artery was introduced. A physiological rate flow was then applied on the system (shear rate 1000 s^{-1}) and 0.2 μm sterile filters allowed gas exchange. Arteries were removed from male Wistar rats (200-250 g, 8 week-old from Janvier Labs - CERJ (Le Genest St Isle, France) and cut in segments 5-7 cm length. A Dex-PBMA or Dex-PBMA_{TAC} stent was then expanded into them (2.5 mm in diameter) and the arteries were placed into the circulating *ex vivo* system. 1/500th of the perfusion medium was taken every day for 6 days. A specific assay was developed to quantify the concentration of TAC released in the collected samples

using an immunoaffinity bead-based flow cytometric test and the xMAP® technologies. Sheep polyclonal anti-TAC from R&D Systems (Abingdon, UK) was covalently coupled to the fluorescent color-coded beads (BDTM Cytometric Bead Array). Before the assay and to control the bead grafting, the beads were incubated with a secondary fluorescent antibody (Rabbit anti-Sheep-FITC) from Pierce (Paris, France). In order to determine TAC concentration, samples were mixed with the previously grafted beads and kept in the dark (2 hours, RT). The captured TAC was detected using specific biotinylated anti-tacrolimus secondary antibody (HyTest LTD). After wash, streptavidin-phycoerythrin (PE) detection reagent was incubated with capture bead in the dark (15 min, RT). The acquisition was achieved on BD FACS array bio-analyzer from BD Bioscience (San Jose, CA, USA). The intensity of fluorescence of yellow parameter (PE emits at 585 nm) is proportional to the amount of TAC present in samples. Standard curves of TAC (range 48-25,000 pg.ml⁻¹) were run in each assay.

In vivo implantation

The procedures and the animal care complied with the “Principles of animal care” formulated by the European Union (Animal Facility Agreement n°75-18-03, 2005) and the protocol was approved by the ethical committee (authorization n°75-214, French Ministry of Agriculture).

Rat intramuscular and intra-aortic implantations

Twelve healthy male Wistar rats (9 to 11 week-old, CERJ, France) were used for the study. The rats were sedated before and during each manipulation with Pentobarbital (0.1% v/w).

Intramuscular implantation: Foreign body reaction to Dex-PBMA was first evaluated by intramuscular implantation. Dex-PBMA films were implanted in the abdominal wall of 9-weeks-old male Wistar rats and harvested after 7 and 30 days (n=3). After 48h of immersion fixation with 4% formalin, tissues were embedded with paraffin. Sections of 6 µm thickness were cut (Microm HM) from the middle part of the film, then deparaffined and stained with hematoxylin-eosin (HE) and Naphthol AS-D Chloroacetate esterase stains. The thickness of the cell cap was measured 5 times on HE histological sections, 3 sections by rats (n=3), using the soft NDP view after scans by Nanozoomer from Hamamatsu (Hamamatsu City, Japan).

Intra-aortic implantation. Dex-PBMA stent coating was then evaluating. 11-weeks-old male Wistar rats received a standard diet and aspirin in water (1 mg.mL⁻¹) 72 hours before implantation to sacrifice. A 2.25 mm-diameter 8-mm-long stent was implanted through an abdominal aorta access. After a flush of the aorta with 200 U of heparin sodium from Pfizer (Paris, France), rats were sutured. An angiography was made after 30 days followed by sacrifice. Stented aortas were then harvested, fixed 72 hours with 4% formalin and methyl methacrylate-embedded (Sigma,

France) protocol adapted from Rippstein et al.³⁰ Section of 10 µm thickness were cut from the middle part of the stent. Subsequently, sections were deplastified and stained with HE or immune-stained with alpha actin, RECA (endothelial cells) and CD-68 (macrophages - respectively MCA5781GA, clone HIS52 Bio-Rad and MCA341GA from Bio-Rad AbD Serotec (Kidlington, UK).

Implantation in a rabbit model of intimal hyperplasia

The protocol was adapted from Feldman et al.³¹ Three male New Zealand White Rabbits, weighing 3.5 to 4.7 kg, were fed a 0.3% cholesterol diet, started 21 days before angioplasty. Animals were anesthetized with intramuscular ketamine 500 U, Xylazine and Vetranquil (14:8:4 v/v). All animals received heparin (1000 U) within the carotid before angioplasty. A 5F sheath was inserted in the left carotid artery. Intimal hyperplasia was induced by balloon angioplasty followed by stent implantation. Bilateral iliac artery angioplasty was performed with a 2.5-mm-diameter, 20-mm-long angioplasty balloon catheter (3 times 1-minute inflation at 8 atm). A 8-mm-long and 2.75 mm in diameter coated stent mounted over the balloon, was implanted in both iliac arteries immediately after balloon angioplasty (30-second inflation at 10 atm), resulting in frank arterial overstretch (1.2 to 1.3 stent-to-artery ratio). Arterial blood was drawn before angioplasty and at euthanasia. The concentration in TNFα was evaluated before implantation and before sacrifice using Elabscience rabbit TNFα ELISA Kit to study the effect Dex-PBMA or Dex-PBMA_{TAC} on TNFα (Houston, USA).

Morphometric analyses of restenosis

According to Feldman et al.³¹ morphometric analyses were performed using the soft NDP view after scans by Nanozoomer from Hamamatsu (Hamamatsu City, Japan). Measurement of the luminal area as well as 2 areas bounded by the internal and external elastic lamina on HE staining served to compute intimal and media areas. Three indexes of intimal growth were used: intimal area, media area and the ratio between these last ones. This experiment was carried out on rat and rabbit stented arteries.

Statistical analysis

Each experiment was carried in triplicate at least. Data are presented as mean +/- standard deviation. One-way analysis of variance (ANOVA) with Bonferroni's post hoc test was used to examine the significance of results between groups if their number were higher than 2 otherwise *t*-test were used. A value of *P* < 0.05 was accepted as statistically significant.

Results

Dex-PBMA characterization

The synthesis leads to a homogeneous white powder of dextran-graft-polybutylmethacrylate copolymer (Dex-PBMA) soluble in a mixture of THF and water (92:8 v/v). The coatings of Dex-PBMA on a glass coverslip,

CoCr disc and CoCr stent or moulding resulted in a transparent film, homogeneous and without cracks. Dex-PBMA deep-coating of stent covered each strut independently with very few webbing. The stent surface modifications were studied using SEM and contact-angle analysis. As shown Fig. 1A, this coating withstands to the crimping on the balloon and the deployment. After one week of incubation at 37°C and under coronary-like flow conditions, Dex-PBMA coating remained unaltered and showed a uniform polymer surface, neither peeling nor delamination was observed.

The coating wettability was evaluated by measuring water contact angles (Fig. 1B). CoCr is less hydrophobic ($\theta=88.7^\circ \pm 2.2$) than Dex-PBMA with or without Tacrolimus (respectively $\theta=98.5^\circ \pm 0.4$ and $99^\circ \pm 2.9$, $P=0.0078$).

Bacterial adhesion

As shown Fig. 2, *Staphylococcus aureus* was lower on Dex-PBMA than on CoCr (ratio 11, $P<0.005$) and control collagen (ratio 4.5, $P<0.05$). In contrast, more bacteria adhered on CoCr than on control (ratio 4.7, $P<0.005$).

Adhesion of platelets and thrombin generation on Dex-PBMA

In static condition, platelet adhered less on Dex-PBMA (Fig. 3A) than on the positive control collagen (ratio 2.7, $P<0.0001$) or on CoCr (ratio 1.39, $P<0,01$). The SEM images showed less platelet activation on the copolymer than on the bare metal. Non-activated platelets are disk-shaped. Once activated, they first take a spherical shape as observed on Dex-PBMA disk (Fig. 3A) before spreading and giving out extensions such as filopodia that can be observed on CoCr surface.³² In dynamic conditions, no platelet adhered on Dex-PBMA (Fig. 3B). Dex-PBMA coating does not promote platelet adhesion and activation in our experimental conditions.

Thrombin generation was performed on Dex-PBMA

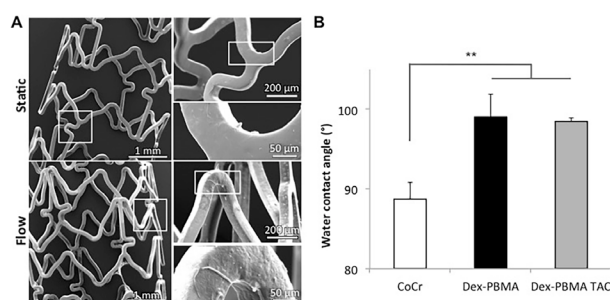


Fig. 1. Dex-PBMA morphology after stent coating. (A) SEM micrographs of dextran grafted poly(butyl methacrylate) (Dex-PBMA) coated stent. Stents were expanded, dip-coated, crimped on a balloon and expanded again. They spend 8 days in water either in static or under flow conditions, shear rate 1000 s^{-1} . (B) Water contact angles on cobalt chrome (CoCr), Dex-PBMA or Dex-PBMA with tacrolimus (Dex-PBMA_{TAC}) discs. Values are mean \pm SEM of 10 determinations ** $P<0,01$.

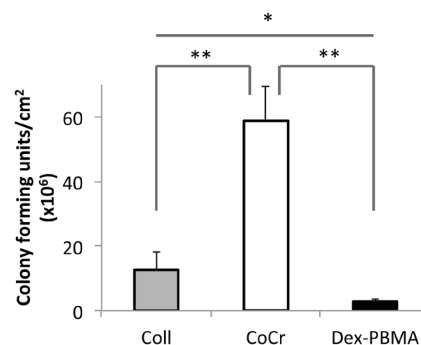


Fig. 2. Bacterial adhesion on Dex-PBMA. Dex-PBMA film, CoCr disc and Collagen (Coll) were incubated 1h incubation at 37°C with a suspension of 108 UFC/mL of *Staphylococcus aureus*. After washing the remaining bacteria were cultivated on agar gel overnight and counted (n=3). Values are mean \pm SEM of three determinations * $P<0,05$; ** $P<0,01$.

and CoCr. In PPP, the velocity index of thrombin generation was 1.9 fold lower on Dex-PBMA disc than on CoCr disc (Fig. 3C, $P<0.01$) in presence of Tissue Factor. There were no differences between the two surfaces for thrombin generation when the assay was performed in PPP without Tissue Factor (Fig. 3C) or in PRP with or without Tissue Factor (data not shown).

Cell adhesion and proliferation onto Dex-PBMA

ECFCs and MSCs adhered less on Dex-PBMA disc than on CoCr disc (Fig. 4). Non-significant differences were obtained for intermediate adhesion (20 min incubation time) whereas for focal adhesion (2 hours incubation time), 2.4 less ECFCs (Fig. 4A, $P<0.0005$) and 1.6 less MSCs (Fig. 4B, $P<0.05$) adhered on Dex-PBMA compared to CoCr discs. The same trends were observed for cell proliferation (Fig. 4C and Fig. 4D). The proliferation of ECFCs and MSCs was greater on CoCr disc than on Dex-PBMA. In both cellular type and surfaces, the proportion of cells compared to control coating of gelatin decrease after 4 days. Thus, CoCr or Dex-PBMA surfaces cause cells to grow more slowly than on control gelatin wells.

Release of tacrolimus from Dex-PBMA

Fig. 5 shows the cumulative TAC release profile from *ex vivo* stented arteries. An extreme burst release was observed corresponding to 5 ng/mL (50%) after 3 hours, followed by a steady state reaching 10 ng/mL over 4 days.

In vivo implantation of Dex-PBMA

Rat intramuscular and intra-aortic implantations

Dex-PBMA films were first implanted in rat abdominal wall to evaluate the tissue reactions after 7 and 30 days (Fig. 6). As shown on HE staining (Fig. 6A), a tissue surrounded the film at day 7 with a thickness of $40 \pm 12 \mu\text{m}$ that remain stable at day 30 ($47 \pm 12 \mu\text{m}$). The low level of Naphthol AS-D Chloroacetate staining indicated

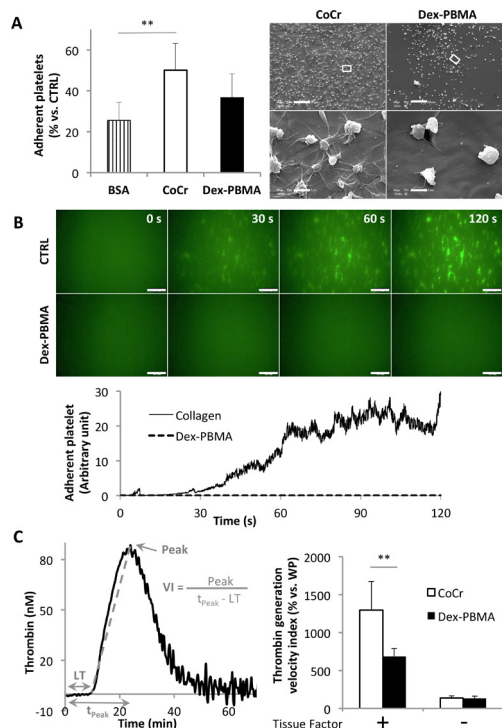


Fig. 3. Human platelet adhesion and thrombin generation onto Dex-PBMA. (A) Left panel: Platelet adhesion in static condition on Dex-PBMA or CoCr discs and bovine serum albumin (BSA, negative control). Quantification of adherent platelets after 2h incubation at room temperature. Data are expressed as a percentage of adherent platelets on collagen (positive control). Values are mean \pm SEM of three determinations. $**P < 0.01$. Right panel: Environmental scanning electron micrographs of adherent platelets on Dex-PBMA and CoCr. Scale bar 20 μ m, higher magnification scale bar 2 μ m. (B) Up: Dynamic adhesion of dioc-6 labeled platelets on Dex-PBMA and collagen coated glass-coverslips submitted to physiological flow (shear rate 1500 s^{-1}). Micrographs of adherent platelets after 0, 30, 60 and 120 s. Down: Quantification of the adhesion within times on Dex-PBMA and collagen. (C) Thrombin generation on Dex-PBMA and CoCr discs. Left panel: Representative curve obtained after a thrombin generation experiment. Parameters of thrombin generation are shown: Lagtime (LT in min), time to peak (t_{Peak} in min) and Peak (nM). Right panel: Velocity Indexes ($VI = Peak / (t_{Peak} - LT)$) for thrombin generation in PPP in the absence or presence of TF (1 μ M) on Dex-PBMA and CoCr. Data are expressed as a percentage of the results on well plate (WP). Values are mean \pm SEM of six determinations. $**P < 0.01$.

that no neutrophil granulocytes were detected in the tissue (Fig. 6B). The capsule is thus mainly composed by collagen without any evidence of inflammatory reaction or necrosis.

Dex-PBMA was then evaluated on a coated stent in rat abdominal aorta. Immediately after implantation, no acute thrombosis was observed. After 30 days, all Dex-PBMA or control CoCr stent implanted rats ($n=6$) survived. At day 30, angiographies confirmed that all arteries were patent. As shown in Fig. 7, no thrombus was found in Dex-PBMA or CoCr stented arteries. Nevertheless, a small intimal hyperplasia was observed both on Dex-PBMA and CoCr

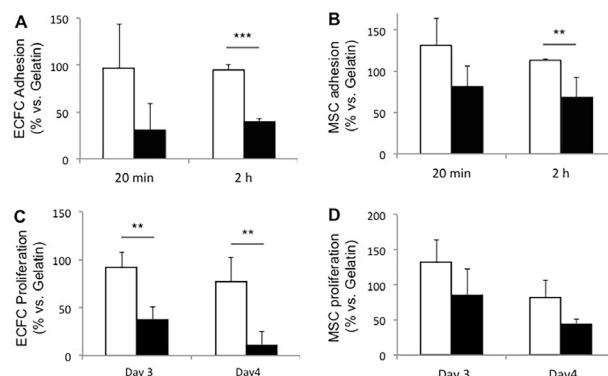


Fig. 4. Circulating cells adhesion and proliferation on Dex-PBMA. (A-B) Human endothelial colony-forming cells (ECFCs) (A) and mesenchymal stem cells (MSCs) (B) intermediate (20 min) and focal (2 h) adhesion on Dex-PBMA (black bar) and CoCr (white bar) discs. (C-D) ECFCs (C) and MSCs (D) proliferations after 72h (day 3) and 96h (day 4) of culture. Data are expressed as a percentage of the positive control: gelatin. Values are mean \pm SEM of 3 determinations. $***P < 0.001$, $**P < 0.01$.

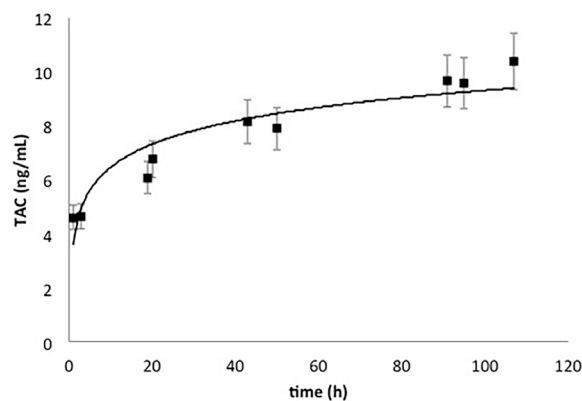


Fig. 5. Ex vivo cumulative Tacrolimus release profile from rat abdominal aorta stented with Dex-PBMA_{TAC} stent for a period of 2 hours in perfusion medium at 37°C under flow conditions (shear rate 1000 s^{-1}).

stents whereas no significant differences were noticed in the areas of intima (0.54 ± 0.007 mm^2 vs. 0.50 ± 0.06 mm^2) and media (0.40 ± 0.04 mm^2 vs. 0.43 ± 0.02 mm^2) on CoCr stent and Dex-PBMA stent (Fig. 7A). No macrophages were emphasized in the arterial wall (CD 68 staining, Fig. 7B). The neointima was mainly composed of SMCs (α -actin staining). This SMC layer was covered by an endothelial layer (RECA staining) on Dex-PBMA as well on CoCr stents (Fig. 7B). As observed *in vitro*, no platelets adhered on Dex-PBMA and we noticed the absence of thrombus formation.

Implantation in a rabbit model of intimal hyperplasia

Dex-PBMA or Dex-PBMA_{TAC} stents were evaluated in a pathological model of neointimal hyperplasia. After 30 days the iliac arteries were patent. Hematoxylin-eosin staining indicated a neointima (Fig. 8A). The measurements emphasized a higher ratio of intima and media areas on Dex-PBMA stent than on CoCr stent

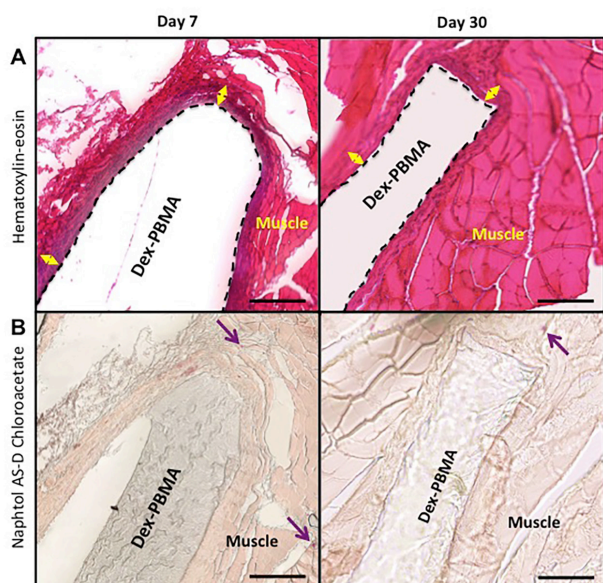


Fig. 6. Histopathologic evaluation for tissue biocompatibility of surrounding tissues after Dex-PBMA intramuscular implantation at 7 and 30 days. (A) Representative photos of hematoxylin-eosin stainings. Double arrows represent cell cap. (B) Granulocytic lineage labeled by naphtol AS-D Chloroacetate esterase staining in purple (arrow). Scale bar 100 µm.

(2.39 vs 1.90). Nevertheless, with Dex-PBMA_{TAC} this ratio decreased (1.60 vs 2.39). On the other hand, TNF-α blood concentration used as a biomarker between before and 30 days after implantation increased in CoCr stent implanted rabbit (+15.6 pg/mL), and remain stable for Dex-PBMA stent implanted rabbit (+0.53 pg/mL) and decreased for Dex-PBMA_{TAC} stent implanted rabbit (-4.87 pg/mL) (Fig. 8B).

Discussion

Implantable medical devices integration is a challenge. Their biocompatibility relates to the specific interaction between the biomaterial, blood components and tissue vessel. In previous studies, we demonstrated that Dex-PBMA polymer coating improves *in vitro* the endothelial cell coverage and limits the SMC proliferation involved in the stent restenosis.^{22,23} Current complications on stent are not only due to stent restenosis but also to LST.^{21,33,34} Both stent geometry and position play a role in stent thrombosis outbreak.^{4,35} Stent coating itself is a major factor in its interactions with blood and vascular wall and its quality can be highly variable.³⁵ Indeed, implanted commercial coated stent showed uncoated areas, craters, webbing or cracks.^{36,37} Coating integrity and mechanical resistance during implantation and indwell have an impact on long-term stent safety.¹⁴ In the present work, Dex-PBMA stent struts were fully and homogeneously coated. The coating resists to both crimping and stent deployment as well as under the shear stress of physiological flow. This behavior prevents polymer fragmentation and

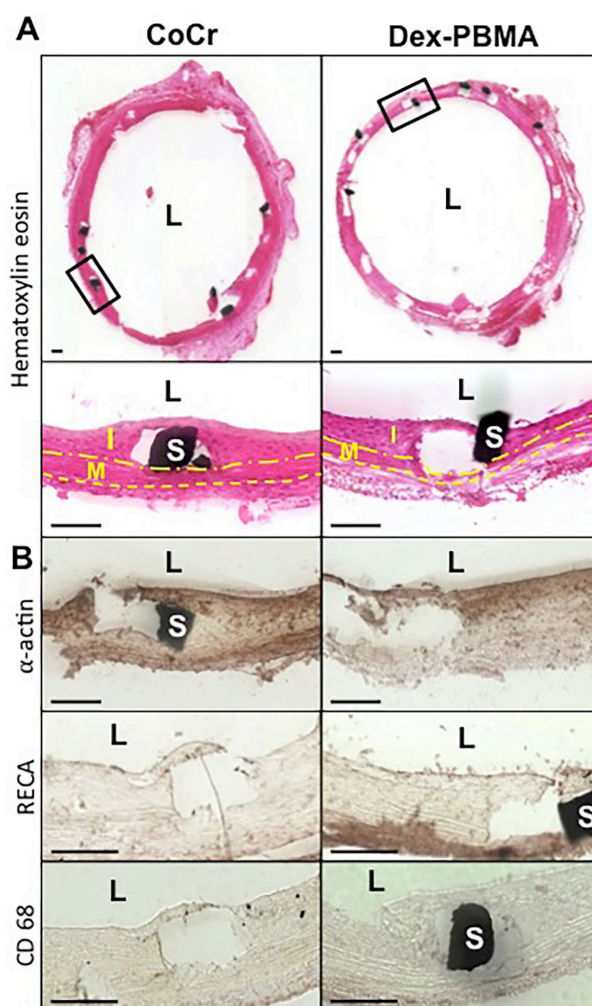


Fig. 7. Dex-PBMA coated or bare CoCr stent implantation in rat abdominal aorta after 30 days. (A) Representative Hematoxylin-Eosin stainings. L indicates the lumen, I the intima delimited by the lumen and internal elastic lamina (dashdotted line), M the media delimited by the internal and the external elastic laminas (dashed line) and S a strut of the stent. (B) Representatives α-actin (smooth muscle cells), RECA (endothelial cells) and CD 68 (Macrophages) immuno-stainings. In both cases, a layer of cell proliferated in lumen. It was formed by SMCs and no macrophages were evident. An endothelium was still present. Scale bar 100 µm.

embolization in blood circulation.

Several studies underline the importance of a rapid re-endothelialization of the stented area.¹⁹ In humans, re-endothelialization is due to the proliferation and migration of adjacent endothelial cells (ECs), but also to the contribution of endothelial progenitors cells in the circulation blood that differentiate in ECs.^{38,39} For instance, anti-CD34-bio-engineered stents were developed to reduce thrombogenicity.^{13,40,41} Because ECFCs that differentiated *in vitro* from endothelial progenitors and MSCs allows wound healing, we thus investigated their adhesion and growth on Dex-PBMA surface. Measurement of cell adhesion, viability and proliferation revealed no cytotoxic effect.

In previous studies, a lower hydrophobic copolymer

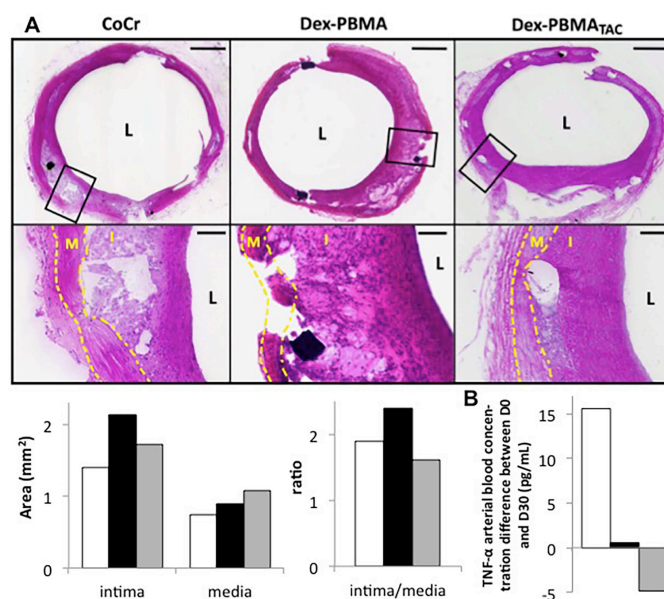


Fig. 8. Dex-PBMA with or without Tacrolimus coated or bare CoCr stent implantation in rabbit iliac artery restenosis model after 30 days ($n=1$, 3 animals, preliminary study). (A) Representative Hematoxylin-Eosin stainings (Up). L indicates the lumen, I the intima delimited by the lumen and internal elastic lamina (dashdotted line) and M the media delimited by the internal and the external elastic lamina (dashed line). Quantification of intimal hyperplasia (down) on Dex-PBMA (black bar), Dex-PBMA_{TAC} (grey bar) and CoCr (white) stents. Comparison of areas of the intima and media and the ratio of these last ones. (B) Difference of TNF α arterial blood concentration between before stent implantation and 30 days later before sacrifice.

of dextran and PBMA ($\theta = 79.4 \pm 0.3$ vs $\theta = 98.5^\circ \pm 0.4$) improves *in vitro* the endothelial cell coverage and limits the SMC proliferation involved in stent restenosis.^{22,23} This difference could be explained by the control of cerium concentration during the synthesis. Because cerium is able to increase prothrombin formation, coagulation time and induce a proinflammatory cytokine secretion,^{42,43} cerium concentration was decreased from 0.2 M to 0.05 M and additional filtration steps were performed. Elementary analysis confirmed the decrease of the residual cerium concentration from $1.73 \pm 0.15\%$ to $0.069 \pm 0.033\%$. The hydrophobicity of Dex-PBMA can explain the observed differences *in vitro*. Numerous works demonstrated the impact of the surface wettability on cell adhesion and proliferation.⁴⁴ Nevertheless, this effect is lowered *in vivo*, by plasmatic protein deposition, mainly the albumin, which occurred immediately after the device implantation,^{45,46} increasing the wettability and favoring the material integration as observed in our *in vivo* study. Indeed, in both rat healthy aorta and rabbit pathological models, hyperplasia on Dex-PBMA stents were limited and comparable to CoCr Stents. Moreover, immunostaining highlighted a new endothelial cell layer in rats.

As the transcatheter way of stent implantation may involve a bacterial infection risk and some lethal cases, bacterial adhesion was evaluated.²⁹ However, dextran is known to favor bacterial adhesion and growth,⁴⁷ and functionalized polymethyl methacrylate-based polymers were shown to prevent it.²⁸ *S. aureus* adhesion to Dex-PBMA CoCr disk was thus assessed and was

equivalent to the negative control. In contrast, a higher rate of bacterial adhesion was observed on bare CoCr disk, probably due to the electropolishing surface treatment used for clinical stent preparation,⁴⁸ which generates micro-scratches favoring bacterial adhesion on the surface. In our experimental conditions, our Dex-PBMA coating was shown to prevent bacterial adhesion.

Hemocompatibility is identified as a key milestone for a vascular device development. Platelet adhesion and blood coagulation are modulated by material surface.⁴⁹⁻⁵¹ As an example, in polylactic acid and magnesium scaffolds or silicone rubbers material used for the biomedical membrane, the thrombosis remains the main complication.^{35,52,53} The Platelet adhesion was thus evaluated as reflect of primary hemostasis. We studied either *in vitro* static and dynamic platelets adhesion as well as thrombin generation on Dex-PBMA surfaces. In static and dynamic conditions few platelets adhered on the surface coated with Dex-PBMA as compared to the bare metal CoCr. We then quantify thrombin generation, which allows us to check the influence of our copolymer on all the coagulation pathways. Dex-PBMA copolymer reduces the formation of thrombin in plasma when coated on CoCr, reflecting an inhibition of the coagulation pathway. Thus, our results showed that Dex-PBMA copolymer is hemocompatible and do not trigger platelets adhesion and activation, as well as blood coagulation.

Moreover *in vivo*, both in rat and rabbit models, histological results show the absence of acute thrombosis immediately after the implantation or at the time of

explanation. Therefore Dex-PBMA exhibits key factors for hemocompatibility.

Since several strategies are currently used to improve the stent efficiency by adding drug in the coating of the whole structure, the abluminal face or by introducing it into the micro-cavities,^{11,54} we investigated the possibility to use dextran-PBMA polymer as a drug delivery platform. Tacrolimus, a macrolide molecule loaded in several stents polymer stent coating,⁸ was chosen as a drug model. Under flow, we demonstrated that Dex-PBMA coating could act as a drug eluting platform and release TAC in the medium. A burst release profile (50%) within 3 hours and a steady state over 4 days were observed. These results show a release profile similar to pharmacokinetic profiles of DESs such as the clinical Janus CarbosStent™ that releases TAC in the vascular wall tissue within the first hours, and then reaches the steady-state within 6 days.^{8,55} The release profile depends on the initial coating as well as the loaded concentration in the stent.⁵⁶ The duration of Tacrolimus release from Dex-PBMA_{TAC} can be improved using multilayer of Dex-PBMA coating strategy as observed with the Cypher^{®21} or the Infinium[®] stents.¹⁵ In our conditions, the low loading level of the drug could explain the results observed *in vivo* in restenosis rabbit model where no difference was seen between Dex-PBMA_{TAC} and Dex-PBMA stents. Another study should be devoted in the future to increase the amount of drug and then evaluate its efficiency.

The *in vivo* implantation of a material and its degradation induce the local repair process, which involves the inflammation and the remodeling process.⁵⁷⁻⁵⁹ From the *in vivo* results, neither esterase staining nor TNF α blood cytokine modification was found. No pathologic inflammatory reaction was observed in the intramuscular position or in the aorta. Furthermore, the fibrous cap thickness is important in the case of drug delivery.⁵⁷ A thicker cap decreases drug release. Dex-PBMA shows a moderate thickness of the fibrous cap as compared to other drug delivery platforms.⁶⁰ Therefore Dex-PBMA can therefore be proposed as an interesting local drug delivery platform.

Conclusion

The present study shows that Dex-PBMA exhibited properties suitable for stent coating, resisted to mechanical forces required for crimping coating processes, remained undamaged under flow conditions and could release a drug. Dex-PBMA exhibited moderate platelet adhesion and did not trigger thrombin generation *in vitro* and allowed endothelial progenitor and MSCs proliferation. *In vivo* Dex-PBMA i) was efficient to promote endothelial coverage 30 days after stent implantation that might prevent side effects in contact with blood, ii) prevented pathological inflammatory reaction in a rabbit model of intimal hyperplasia. Dex-PBMA represents therefore a

Research Highlights

What is the current knowledge?

- ✓ PBMA polymers are used in the commercial stent coating
- ✓ Dex-PBMA with suitable elastic properties were developed as a stent coating.
- ✓ The nature of the polymer coating is involved in the major complications after stent implantation: restenosis and LST.

What is new here?

- ✓ *In vitro* under physiological flow, Dex-PBMA is hemocompatible and do not trigger platelet adhesion and activation as well as blood coagulation
- ✓ Dex-PBMA stent coating remained unaltered and could release Tacrolimus under coronary-like flow conditions.
- ✓ Dex-PBMA exhibits biocompatibility properties *in vivo* in aortic stent rat model and in pathological neointimal hyperplasia rabbit model.

new opportunity and an interesting alternative for coating implantable medical devices at the interface with the blood.

Acknowledgments

Cecilia Delattre would like to thank the Groupe de Réflexion sur la Recherche Cardio-vasculaire, the Fédération Française de Cardiologie and the Société Française de Cardiologie for providing a Ph.D. Scholarship. We thank the nursing services of Hôpital St Louis and Bicêtre Hospital for providing umbilical cord blood samples.

Funding sources

This work was supported by the European FP7 program PRESTIGE.

Ethical Statement

The study was approved by the Biological Resources Center in the Cell Therapy Unit from Saint Louis Hospital (Paris, France), authorized by French Ministry of Research under number AC-2008-376 and certified by the French Normalization Agency under number 201/51848.1. The protocol complied with the Declaration of Helsinki. Umbilical cord blood was collected after normal full-term deliveries with the written informed consent of the mother, and used within 24h.

The *in vivo* procedures and the animal care complied with the “Principles of animal care” formulated by the European Union (Animal Facility Agreement n°75-18-03, 2005) and the protocol was approved by the ethical committee (authorization n°75-214, French Ministry of Agriculture).

Competing interests

The authors declare that the research was conducted in the absence of any commercial or financial relationships that could be construed as a potential conflict of interest.

Authors contribution

The conception and design were performed by CD, GPD, CBV, DL and AMP; financial support was obtained by CR; the collection and/or assembly of data was conducted by CD, DV, CR, VO, AL, TA, VG and AMP; data analysis and interpretation were performed by CD, DV, GPD, VO, TA, GC, MJP, CBV and AMP; and the manuscript was prepared by CD, GPD, CBV, DL and AMP; all authors approved and revised critically the manuscript; and given final approval by AMP.

References

- Katz G, Harchandani B, Shah B. Drug-eluting stents: the past, present, and future. *Curr Atheroscler Rep* **2015**; 17: 485. doi:10.1007/s11883-014-0485-2
- Curcio A, Torella D, Indolfi C. Mechanisms of smooth muscle cell proliferation and endothelial regeneration after vascular injury and stenting: approach to therapy. *Circ J* **2011**; 75: 1287-96. doi:10.1253/circj.CJ-11-0366
- McFadden EP, Stabile E, Regar E, Cheneau E, Ong AT, Kinnaird T, et al. Late thrombosis in drug-eluting coronary stents after discontinuation of antiplatelet therapy. *Lancet* **2004**; 364: 1519-21. doi:10.1016/S0140-6736(04)17275-9
- Serruys PW, Daemen J. Are drug-eluting stents associated with a higher rate of late thrombosis than bare metal stents? Late stent thrombosis: a nuisance in both bare metal and drug-eluting stents. *Circulation* **2007**; 115: 1433-9; discussion 9. doi:10.1161/CIRCULATIONAHA.106.666826
- Joner M, Nakazawa G, Finn AV, Quee SC, Coleman L, Acampado E, et al. Endothelial cell recovery between comparator polymer-based drug-eluting stents. *J Am Coll Cardiol* **2008**; 52: 333-42. doi:10.1016/j.jacc.2008.04.030
- Virmani R, Guagliumi G, Farb A, Musumeci G, Grieco N, Motta T, et al. Localized hypersensitivity and late coronary thrombosis secondary to a sirolimus-eluting stent: should we be cautious? *Circulation* **2004**; 109: 701-5. doi:10.1161/01.CIR.0000116202.41966.D4
- Puranik AS, Dawson ER, Peppas NA. Recent advances in drug eluting stents. *Int J Pharm* **2013**; 441: 665-79. doi:10.1016/j.ijpharm.2012.10.029
- Bartorelli AL, Trabattini D, Fabbicchi F, Montorsi P, de Martini S, Calligaris G, et al. Synergy of passive coating and targeted drug delivery: the tacrolimus-eluting Janus CarboStent. *J Interv Cardiol* **2003**; 16: 499-505. doi:10.1046/j.1540-8183.2003.01050.x
- Charbonneau C, Ruiz JC, Lequoy P, Hebert MJ, De Crescenzo G, Wertheimer MR, et al. Chondroitin sulfate and epidermal growth factor immobilization after plasma polymerization: a versatile anti-apoptotic coating to promote healing around stent grafts. *Macromol Biosci* **2012**; 12: 812-21. doi:10.1002/mabi.201100447
- Khan W, Farah S, Domb AJ. Drug eluting stents: developments and current status. *J Control Release* **2012**; 161: 703-12. doi:10.1016/j.jconrel.2012.02.010
- Garg S, Serruys PW. Coronary stents: looking forward. *J Am Coll Cardiol* **2010**; 56: S43-78. doi:10.1016/j.jacc.2010.06.008
- Raber L, Serruys PW. Late vascular response following drug-eluting stent implantation. *JACC Cardiovasc Interv* **2011**; 4: 1075-8. doi:10.1016/j.jcin.2011.06.016
- Abizaid A, Costa JR, Jr. New drug-eluting stents: an overview on biodegradable and polymer-free next-generation stent systems. *Circ Cardiovasc Interv* **2010**; 3: 384-93. doi:10.1161/CIRCINTERVENTIONS.109.891192
- Navarro L, Mogosanu DE, de Jong T, Bakker AD, Schaubroeck D, Luna J, et al. Poly(polyol sebacate) Elastomers as Coatings for Metallic Coronary Stents. *Macromol Biosci* **2016**; 16: 1678-92. doi:10.1002/mabi.201600105
- Sun D, Zheng Y, Yin T, Tang C, Yu Q, Wang G. Coronary drug-eluting stents: From design optimization to newer strategies. *J Biomed Mater Res A* **2014**; 102: 1625-40. doi:10.1002/jbm.a.34806
- Cha KJ, Lih E, Choi J, Joung YK, Ahn DJ, Han DK. Shape-memory effect by specific biodegradable polymer blending for biomedical applications. *Macromol Biosci* **2014**; 14: 667-78. doi:10.1002/mabi.201300481
- Moravej M, Mantovani D. Biodegradable metals for cardiovascular stent application: interests and new opportunities. *Int J Mol Sci* **2011**; 12: 4250-70. doi:10.3390/ijms12074250
- Svedman C, Moller H, Gruvberger B, Gustavsson CG, Dahlin J, Persson L, et al. Implants and contact allergy: are sensitizing metals released as haptens from coronary stents? *Contact Dermatitis* **2014**; 71: 92-7. doi:10.1111/cod.12242
- Kipshidze N, Dangas G, Tsapenko M, Moses J, Leon MB, Kutryk M, et al. Role of the endothelium in modulating neointimal formation: vasculoprotective approaches to attenuate restenosis after percutaneous coronary interventions. *J Am Coll Cardiol* **2004**; 44: 733-9. doi:10.1016/j.jacc.2004.04.048
- Hu T, Yang J, Cui K, Rao Q, Yin T, Tan L, et al. Controlled Slow-Release Drug-Eluting Stents for the Prevention of Coronary Restenosis: Recent Progress and Future Prospects. *ACS Appl Mater Interfaces* **2015**; 7: 11695-712. doi:10.1021/acsami.5b01993
- Garg S, Serruys PW. Coronary stents: current status. *J Am Coll Cardiol* **2010**; 56: S1-42. doi:10.1016/j.jacc.2010.06.007
- Derkaoui SM, Labbe A, Chevallier P, Holvoet S, Roques C, Avramoglou T, et al. A new dextran-graft-polybutylmethacrylate copolymer coated on 316L metallic stents enhances endothelial cell coverage. *Acta Biomater* **2012**; 8: 3509-15. doi:10.1016/j.actbio.2012.05.030
- Derkaoui SM, Labbe A, Purnama A, Gueguen V, Barbaud C, Avramoglou T, et al. Films of dextran-graft-polybutylmethacrylate to enhance endothelialization of materials. *Acta Biomater* **2010**; 6: 3506-13. doi:10.1016/j.actbio.2010.03.043
- De Groot CJ, Van Luyn MJ, Van Dijk-Wolthuis WN, Cadee JA, Plantinga JA, Den Otter W, et al. In vitro biocompatibility of biodegradable dextran-based hydrogels tested with human fibroblasts. *Biomaterials* **2001**; 22: 1197-203. doi.org/10.1016/S0142-9612(00)00266-0
- Jandrot-Perrus M, Lagrue AH, Okuma M, Bon C. Adhesion and activation of human platelets induced by convulxin involve glycoprotein VI and integrin alpha2beta1. *J Biol Chem* **1997**; 272: 27035-41. doi: 10.1074/jbc.272.43.27035
- Zemani F, Silvestre JS, Fauvel-Lafeve F, Bruel A, Vilar J, Bieche I, et al. Ex vivo priming of endothelial progenitor cells with SDF-1 before transplantation could increase their proangiogenic potential. *Arterioscler Thromb Vasc Biol* **2008**; 28: 644-50. doi:10.1161/ATVBAHA.107.160044
- Ino JM, Sju E, Ollivier V, Yim EK, Letourneur D, Le Visage C. Evaluation of hemocompatibility and endothelialization of hybrid poly(vinyl alcohol) (PVA)/gelatin polymer films. *J Biomed Mater Res B Appl Biomater* **2013**; 101: 1549-59. doi:10.1002/jbm.b.32977
- Anagnostou F, Debet A, Pavon-Djavid G, Goudaby Z, Helary G, Migonney V. Osteoblast functions on functionalized PMMA-based polymers exhibiting Staphylococcus aureus adhesion inhibition. *Biomaterials* **2006**; 27: 3912-9. doi:10.1016/j.biomaterials.2006.03.004
- Bosman WM, Borger van der Burg BL, Schuttevaer HM, Thoma S, Hedeman Joosten PP. Infections of intravascular bare metal stents: a case report and review of literature. *Eur J Vasc Endovasc Surg* **2014**; 47: 87-99. doi:10.1016/j.ejvs.2013.10.006
- Rippstein P, Black MK, Boivin M, Veinot JP, Ma X, Chen YX, et al. Comparison of processing and sectioning methodologies for arteries containing metallic stents. *J Histochem Cytochem* **2006**; 54: 673-81. doi:10.1369/jhc.5A6824.2006
- Feldman LJ, Aguirre L, Zioli M, Bridou JP, Nevo N, Michel JB, et al. Interleukin-10 inhibits intimal hyperplasia after angioplasty or stent implantation in hypercholesterolemic rabbits. *Circulation* **2000**; 101: 908-16. doi.org/10.1161/01.CIR.101.8.908
- Zucker MB, Nachmias VT. Platelet activation. *Arteriosclerosis*

- 1985**; 5: 2-18. doi:10.1161/01.ATV.5.1.2
33. Hara H, Nakamura M, Palmaz JC, Schwartz RS. Role of stent design and coatings on restenosis and thrombosis. *Adv Drug Deliv Rev* **2006**; 58: 377-86. doi:10.1016/j.addr.2006.01.022
 34. Iakovou I, Schmidt T, Bonizzoni E, Ge L, Sangiorgi GM, Stankovic G, et al. Incidence, predictors, and outcome of thrombosis after successful implantation of drug-eluting stents. *JAMA* **2005**; 293: 2126-30. doi:10.1001/jama.293.17.2126
 35. Foin N, Lee RD, Torii R, Guitierrez-Chico JL, Mattesini A, Nijjer S, et al. Impact of stent strut design in metallic stents and biodegradable scaffolds. *Int J Cardiol* **2014**; 177: 800-8. doi:10.1016/j.ijcard.2014.09.143
 36. Basalus MW, Tandjung K, van Westen T, Sen H, van der Jagt PK, Grijpma DW, et al. Scanning electron microscopic assessment of coating irregularities and their precursors in unexpanded durable polymer-based drug-eluting stents. *Catheter Cardiovasc Interv* **2012**; 79: 644-53. doi:10.1002/ccd.23273
 37. Wiemer M, Butz T, Schmidt W, Schmitz KP, Horstkotte D, Langer C. Scanning electron microscopic analysis of different drug eluting stents after failed implantation: from nearly undamaged to major damaged polymers. *Catheter Cardiovasc Interv* **2010**; 75: 905-11. doi:10.1002/ccd.22347
 38. Fioretta ES, Fledderus JO, Burakowska-Meise EA, Baaijens FP, Verhaar MC, Bouten CV. Polymer-based scaffold designs for in situ vascular tissue engineering: controlling recruitment and differentiation behavior of endothelial colony forming cells. *Macromol Biosci* **2012**; 12: 577-90. doi:10.1002/mabi.201100315
 39. Hagensen MK, Vanhoutte PM, Bentzon JF. Arterial endothelial cells: still the craftsmen of regenerated endothelium. *Cardiovasc Res* **2012**; 95: 281-9. doi:10.1093/cvr/cvs182
 40. Larsen K, Cheng C, Tempel D, Parker S, Yazdani S, den Dekker WK, et al. Capture of circulatory endothelial progenitor cells and accelerated re-endothelialization of a bio-engineered stent in human ex vivo shunt and rabbit denudation model. *Eur Heart J* **2012**; 33: 120-8. doi:10.1093/eurheartj/ehr196
 41. Inoue T, Croce K, Morooka T, Sakuma M, Node K, Simon DI. Vascular inflammation and repair: implications for re-endothelialization, restenosis, and stent thrombosis. *JACC Cardiovasc Interv* **2011**; 4: 1057-66. doi:10.1016/j.jcin.2011.05.025
 42. Graca JG, Davison FC, Feavel JB. Comparative Toxicity of Stable Rare Earth Compounds. Iii. Acute Toxicity of Intravenous Injections of Chlorides and Chelates in Dogs. *Arch Environ Health* **1964**; 8: 555-64.
 43. Pagano G, Guida M, Tommasi F, Oral R. Health effects and toxicity mechanisms of rare earth elements-Knowledge gaps and research prospects. *Ecotoxicol Environ Saf* **2015**; 115: 40-8. doi:10.1016/j.ecoenv.2015.01.030
 44. Kim SH, Ha HJ, Ko YK, Yoon SJ, Rhee JM, Kim MS, et al. Correlation of proliferation, morphology and biological responses of fibroblasts on LDPE with different surface wettability. *J Biomater Sci Polym Ed* **2007**; 18: 609-22. doi:10.1163/156856207780852514
 45. Baier RE, Dutton RC. Initial events in interactions of blood with a foreign surface. *J Biomed Mater Res* **1969**; 3: 191-206. doi:10.1002/jbm.820030115
 46. Wilson CJ, Clegg RE, Leavesley DI, Percy MJ. Mediation of biomaterial-cell interactions by adsorbed proteins: a review. *Tissue Eng* **2005**; 11: 1-18. doi:10.1089/ten.2005.11.1
 47. Vaudaux P, Avramoglou T, Letourneur D, Lew DP, Jozefonvicz J. Inhibition by heparin and derivatized dextrans of Staphylococcus aureus adhesion to fibronectin-coated biomaterials. *J Biomater Sci Polym Ed* **1992**; 4: 89-97. doi.org/10.1163/156856292X00321
 48. Tepe G, Wendel HP, Khorchidi S, Schmehl J, Wiskirchen J, Pusich B, et al. Thrombogenicity of various endovascular stent types: an in vitro evaluation. *J Vasc Interv Radiol* **2002**; 13: 1029-35.
 49. Antonucci D, Valenti R, Migliorini A, Moschi G, Trapani M, Bolognese L, et al. Clinical and angiographic outcomes following elective implantation of the Carbostent in patients at high risk of restenosis and target vessel failure. *Catheter Cardiovasc Interv* **2001**; 54: 420-6.
 50. Fort S, Kornowski R, Silber S, Lewis BS, Bilodeau L, Almagor Y, et al. 'Fused-Gold' vs. 'Bare' stainless steel NIRflex stents of the same geometric design in diseased native coronary arteries. Long-term results from the NIR TOP Study. *EuroIntervention* **2007**; 3: 256-61. DOI: 10.4244/EIJV3I2A44
 51. Gutensohn K, Beythien C, Bau J, Fenner T, Grewe P, Koester R, et al. In vitro analyses of diamond-like carbon coated stents. Reduction of metal ion release, platelet activation, and thrombogenicity. *Thromb Res* **2000**; 99: 577-85. doi:10.1016/S0049-3848(00)00295-4
 52. Caiazzo G, Kilic ID, Fabris E, Serdoz R, Mattesini A, Foin N, et al. Absorbable bioresorbable vascular scaffold: What have we learned after 5years of clinical experience? *Int J Cardiol* **2015**; 201: 129-36. doi:10.1016/j.ijcard.2015.07.101
 53. Rao H, Zhang Z, Liu F. Enhanced mechanical properties and blood compatibility of PDMS/liquid crystal cross-linked membrane materials. *J Mech Behav Biomed Mater* **2013**; 20: 347-53. doi:10.1016/j.jmbbm.2013.01.010
 54. Mennuni MG, Pagnotta PA, Stefanini GG. Coronary Stents: The Impact of Technological Advances on Clinical Outcomes. *Ann Biomed Eng* **2015**. doi:10.1007/s10439-015-1399-z
 55. Naseerali CP, Hari PR, Sreenivasan K. The release kinetics of drug eluting stents containing sirolimus as coated drug: role of release media. *J Chromatogr B Analyt Technol Biomed Life Sci* **2010**; 878: 709-12. doi:10.1016/j.jchromb.2010.01.023
 56. Papafaklis MI, Chatzizisis YS, Naka KK, Giannoglou GD, Michalis LK. Drug-eluting stent restenosis: effect of drug type, release kinetics, hemodynamics and coating strategy. *Pharmacol Ther* **2012**; 134: 43-53. doi:10.1016/j.pharmthera.2011.12.006
 57. Anderson JM, Rodriguez A, Chang DT. Foreign body reaction to biomaterials. *Semin Immunol* **2008**; 20: 86-100. doi:10.1016/j.smim.2007.11.004
 58. Lewis F, Cloutier M, Chevallier P, Turgeon S, Pireaux JJ, Tatoulian M, et al. Influence of the 316 L stainless steel interface on the stability and barrier properties of plasma fluorocarbon films. *ACS Appl Mater Interfaces* **2011**; 3: 2323-31. doi:10.1021/am200245d
 59. Catelas I, Wimmer MA, Utzschneider S. Polyethylene and metal wear particles: characteristics and biological effects. *Semin Immunopathol* **2011**; 33: 257-71. doi:10.1007/s00281-011-0242-3
 60. Park S, Park M, Kim BH, Lee JE, Park HJ, Lee SH, et al. Acute suppression of TGF-ss with local, sustained release of tranilast against the formation of fibrous capsules around silicone implants. *J Control Release* **2015**; 200: 125-37. doi:10.1016/j.jconrel.2014.12.021